ACS Sustainable Chemistry & Engineering

Research Article

pubs.acs.org/journal/ascecg

Morphology Control of TiO_2 Nanoparticle in Microemulsion and Its Photocatalytic Property

Xiangcun Li,* Wenji Zheng, Gaohong He,* Rui Zhao, and Dan Liu

State Key Laboratory of Fine Chemicals, The R&D Center of Membrane Science and Technology, School of Chemical Engineering, Dalian University of Technology, No. 2 Linggong Road, Ganjingzi District, Dalian City, Liaoning Province, P. R. China 116024

Supporting Information

ABSTRACT: TiO_2 nanoparticles with controlled morphology and high photoactivity were prepared using a microemulsion-mediated hydrothermal method in this study, and the particles were characterized by means of TEM, XRD, BET, and BJH analysis. As the hydrothermal temperature is elevated, mean pore diameter, crystalline size, and crystallinity of the particles increase gradually, while the surface area decreases significantly, and the morphology changes from a spherical into a rod-like shape. The morphology transition mechanism of the TiO_2 crystal has been put forward based on a decrease in intensity of the microemulsion interface and an increase in collision efficiency between droplets with increasing the hydrothermal temperature. The photocatalytic activity of the TiO_2 particles synthesized at 120−200 °C is relatively low due to their weak crystallinity, though they have high surface area of 146−225 m^2/g and small crystalline size of 6−10 nm. However, the TiO_2 samples prepared at 250−350 °C with low surface area (28−90 m^2/g) exhibit high activity on the degradation of Rhodamine B (RhB), which is comparable or higher than that of the commercial P-25. The reason is ascribed to their high crystallinity that determines material activity in this temperature region. This study reveals that the effects of the surface area, crystallinity, and crystalline size on TiO_2 activity are interdependent, and the balance between these factors is important for improving the photoactivity of the catalyst.

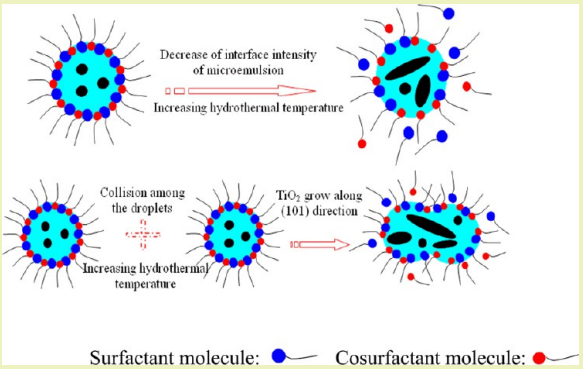

KEYWORDS: *Microemulsion, TiO_2, Photoactivity, Hydrothermal, Crystallinity*

INTRODUCTION

TiO_2 has been accepted as an effective photocatalyst for the photooxidation of different kinds of hazardous organic pollutants in wastewater, drinking water, and air[1−6] because of its nontoxicity, chemical stability, and convenient band gap energy (3.2 eV). The photocatalytic activity of TiO_2 is largely determined by its properties such as specific surface area, crystallinity, crystalline size, and porous structure.[7−10] High photoactivity is associated with crystalline size, and small crystalline size can cause a quantum-sized effect and enhance photoenergy absorption in semiconductors. In addition, TiO_2 materials with a large surface area and high crystallinity always demonstrate enhanced activity for the degradation of environmental contaminants[11−13] because the large surface area can provide many active sites for adsorption of substances, and the high crystallinity can reduce the recombination ratio of the photogenerated electrons and positive holes. Hence, increasing the specific surface area and crystallinity are considered as two effective approaches to improve the photocatalytic activity of TiO_2. However, synthesis of TiO_2 crystals with these two enhanced parameters simultaneously is not always available due to the agglomeration and phase transition of the materials during heat treatment at high temperature. Therefore, it is imperative to study the relationship of the two factors and their synergetic effects on photoactivity of TiO_2.

Recently, various synthesis methods, including the sol−gel hydrolysis process,[14,15] microemulsion and reverse micelles,[16,17] hydrothermal treatment,[18−20] chemical vapor deposition,[21] electrodeposition, and the microwave method,[22−24] have been explored to prepare TiO_2 nanomaterials with different kinds of structures and applications. Especially, microemulsion (reverse micelle) synthesis of oxide materials has been demonstrated to be a very promising method due to its precise control on morphology and dimension of nanoparticles.[25] The surfactant-stabilized microcavity in microemulsion can provide a nanoscale reactor that limits nucleation, growth, and agglomeration of the particles. However, TiO_2 nanoparticles prepared by the microemulsion method always show low photocatalytic activity because of their weak crystallinity. Calcination of the amorphous materials at elevated temperature should be performed in order to improve the activity, but the heat treatment results in TiO_2 nanoparticle sintering, agglomeration, or phase transition from anatase to rutile. TiO_2 nanoparticles

Received: September 5, 2013
Revised: October 18, 2013
Published: October 22, 2013

with high crystallinity have been obtained using he hydrothermal method at a relatively low temperature (~250 °C) without post-treatment.[18,26] Accordingly, a microemulsion−hydrothermal combined technique has been developed for synthesizing anatase-type titania recently.[11,27−30] The influences of water content and pH value in microemulsion, microemulsion composition, and post-heat treatment temperature on crystalline phase, crystalline size, specific surface area, morphology, and photocatalytic activity of TiO_2 nanoparticles have been investigated in previous reports.

In this study, we report the preparation and characterization of mesoporous TiO_2 nanoparticles by the microemulsion-mediated hydrothermal method, mainly focusing on the effects of hydrothermal temperature as well as the microemulsion interface on the morphology, surface area, crystallinity, and photoactivity of the TiO_2 nanoparticles. Compared with the previous results, the formation mechanism of TiO_2 nanoparticles with different morphology and photoactivity has been proposed based on the decrease in intensity of the microemulsion interface and the increase in collision frequency between droplets with increasing the hydrothermal temperature. The synergetic effects of surface area and crystallinity on TiO_2 photoactivity have been discussed. The work provides an alternative approach and novel understanding for preparation of nanomaterials with well-defined morphology and high photocatalytic activity.

EXPERIMENTAL SECTION

Materials and Methods. Titanium isopropoxide (TIP), polyoxyethylene tert-octylphenyl ether (TritonX-100), heptane, hexanol, and all of other chemical reagents were purchased from Sigma-Aldrich and were used without further treatment.

In a typical synthesis of TiO_2 nanoparticles, the microemulsion solution was prepared first by adding the desired amount of TritonX-100 and deionized water into a 5 mL mixture solution of heptane and hexanol (mole ratio 3:1). The concentrations of the surfactant and water in microemulsion solution were 0.20 mol L^{-1} and $W = 56$ ($W = C_{H_2O}/C_{TritonX-100}$), respectively. Then, 1 mL TIP was added dropwise to the microemulsion solution. Subsequently, the resulting solution was transferred into a Teflon-lined 10 mL autoclave and was sealed tightly, and then it was put into an oven for hydrothermal treatment at different temperatures for 13 h. After that, the autoclave was cooled naturally to room temperature, and the precipitates were collected by centrifugation at 5000 rpm and washed with water and ethanol several times prior to drying in air at 60 °C.

Owing to the interaction between methylene blue (MB) and TritonX-100 and its sensitivity to the state of water in the polar core of microemulsion, MB was used as a sensitive probe to study the microenvironment in the TritonX-100 microemulsion.[31,32] It is worth noting that with an increase in W, the absorption maximum λ_m of MB at a high wavelength region increases slowly from about 630 to 650 nm, which reaches a stable value at about $W = 56.0$ (Figure S1, Supporting Information). Meanwhile, the absorption maximum band at about 650 nm resembles the absorption band of free MB in pure water (664 nm). The results reveal that the water molecules should lie between the free and bound state of water, and the microemulsion provides a special microenvironment for the reaction process.

Characterization. The morphology and high-resolution structure of TiO_2 nanoparticles were viewed on a transmission electron microscopy operated at 120 kV (TEM, JEOL 2010). The XRD patterns were recorded on a Scitantag XDS 2000 powder diffractometer at a 2θ scan rate of 2°/min (Cu Kα radiation at 1.54 Å). The crystalline size (D) of the nanoparticles was calculated by the Debye−Sherrer formula $D = 0.89\,\lambda/\beta \cos\theta$, where λ is the wavelength of X-rays, β is the full width in radians at half-maximum of diffraction peaks, and θ is the Bragg angle of the X-ray pattern. Nitrogen adsorption−desorption isotherms of the samples were obtained using the Micromeritics ASAP 2010 at 77 K. The specific surface area was calculated using the Barret−Joyner−Halender (BJH) method. The conductivity of microemulsion was measured by a DDS-11A digital conductometer (cell constant 1.0, frequency 50 ± 1 Hz, measurement standard errors ±1.5%, Shanghai Leici Instrument Company) at different temperatures of microemulsion solution.

Photocatalytic Experiment. The photocatalytic activity of TiO_2 nanoparticles was evaluated by its photodegradation rate on Rhodamine B in deionized water. The experiments were performed in a RPR-100 Rayonet Reactor (1.65×10^{16} photons/sec/cm^3), operated at 35 °C. The bulbs produced a strong peak centered at 254 nm. No additional filters were used, and the distance between the sample and the bulbs was about 15 cm. In a typical process, 10 mg of TiO_2 was added to 50 mL of a 1.0×10^{-5} mol L^{-1} Rhodamine B solution and magnetically stirred in the dark for 30 min to achieve adsorption equilibrium between the dye and the catalyst prior to irradiation. The sample was collected every 20 min and was centrifuged to remove the possible TiO_2 particles. Then the concentration of Rhodamine B was determined by its UV−vis adsorption at 553.5 nm (Shimadzu UV 1700), and the degradation rate was calculated.

RESULTS AND DISCUSSION

Crystallinity and Morphology of TiO_2 Nanoparticles. Figure 1 represents XRD patterns of titania nanoparticles

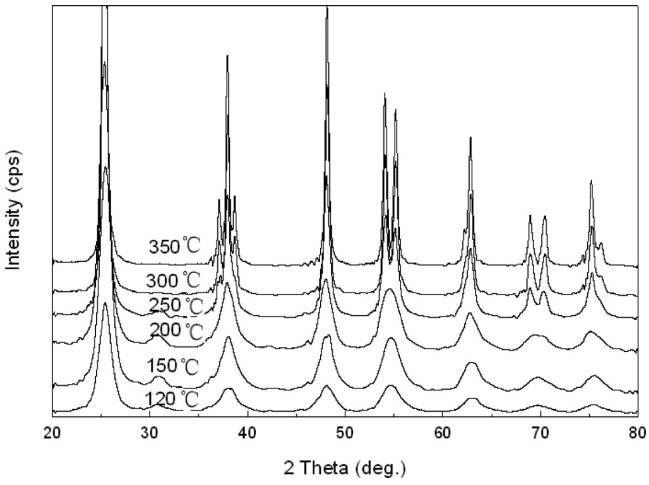

Figure 1. XRD patterns of TiO_2 nanoparticles prepared at different hydrothermal temperatures.

synthesized by the microemulsion method at different hydrothermal temperatures. All of the samples show diffraction peaks well consistent with the data listed in JCPDS card 21-1272, indicating that they are anatase-type titania. In addition, the crystallinity increases with an increase in hydrothermal temperature because higher ordering in the structure of titania particles makes the X-ray peak sharper and more narrow. The strong and narrow peaks also reveal an increase in grain size of TiO_2 powders. The average crystalline size of TiO_2 nanoparticles with anatase phase can be calculated by applying the Debye−Scherrer equation to the anatase (101) diffraction peak as shown in Table 1. The TiO_2 crystalline size increases from 8.10 to 24.33 with an increase in hydrothermal temperature from 120 to 350 °C. This is attributed to a decrease in rigidity and intensity of the microemulsion interface with enhancing the reaction temperature, which reduces the restricting effect of the microemulsion interface on the nuclei growth of TiO_2. Also, the high growing velocity of the crystal at elevated temperature

dx.doi.org/10.1021/sc400328u | ACS Sustainable Chem. Eng. 2014, 2, 288−295

Table 1. Physicochemical Properties of TiO_2 Samples from N_2 Desorption Analysis and XRD Results, Effect of Different Water Contents (1 mL TIP, 120°C for 13 h)

items	S_{BET} (m^2/g)	V (cm^3/g)	D_{BJH} (Å)	crystalline size (nm)	kinetic constant (min^{-1})
W = 11	229.49	0.445	59.66	8.1	0.0292
W = 22	209.87	0.439	64.09	8.5	0.0165
W = 33	225.26	0.443	61.14	8.9	0.0355
W = 44	223.97	0.443	61.41	9.0	0.0351
W = 50	225.13	0.456	81.01	8.7	0.0452

should be responsible for the gradual increase in crystalline size of the TiO_2 nanoparticles. The morphology and particle size of the nanoparticles are further studied by TEM analysis, as shown in Figure 2. In the relative low-temperature range of 120−200 °C, spherical nanoparticles with diameters of 6−10 nm are obtained (Figure 2 a−c), while mixtures of spherical and rod-like-shaped particles are prepared in the temperature range of 250−350 °C (Figure 2 d−f), and the percentage of rod-like-shaped particles is estimated to be about 23.2%, 41.0%, and 58.3% from Figure 2d, e, and f respectively. The results indicate that more spherical particles grow into rod-like ones along their preferred (101) direction with an increase in hydrothermal temperature (Figure 2g and h),[27] further confirming that the microemulsion droplet provides a large space for nuclei growth of TiO_2 because of a decrease in the interface strength at high temperature. The clear lattice image and selected-area electron diffraction (Figure 2i) demonstrates that anatase titania is obtained. These results suggest that the morphology and crystallinity of TiO_2 nanoparticles can be well controlled in this study. To further study the roles of microemulsion and hydrothermal treatment in the formation of TiO_2 particles, titania materials are also prepared by different calcination methods. It is found that the morphology of TiO_2 catalyst cannot be well controlled without the presence of the microemulsion or hydrothermal process (Figure S2, Supporting

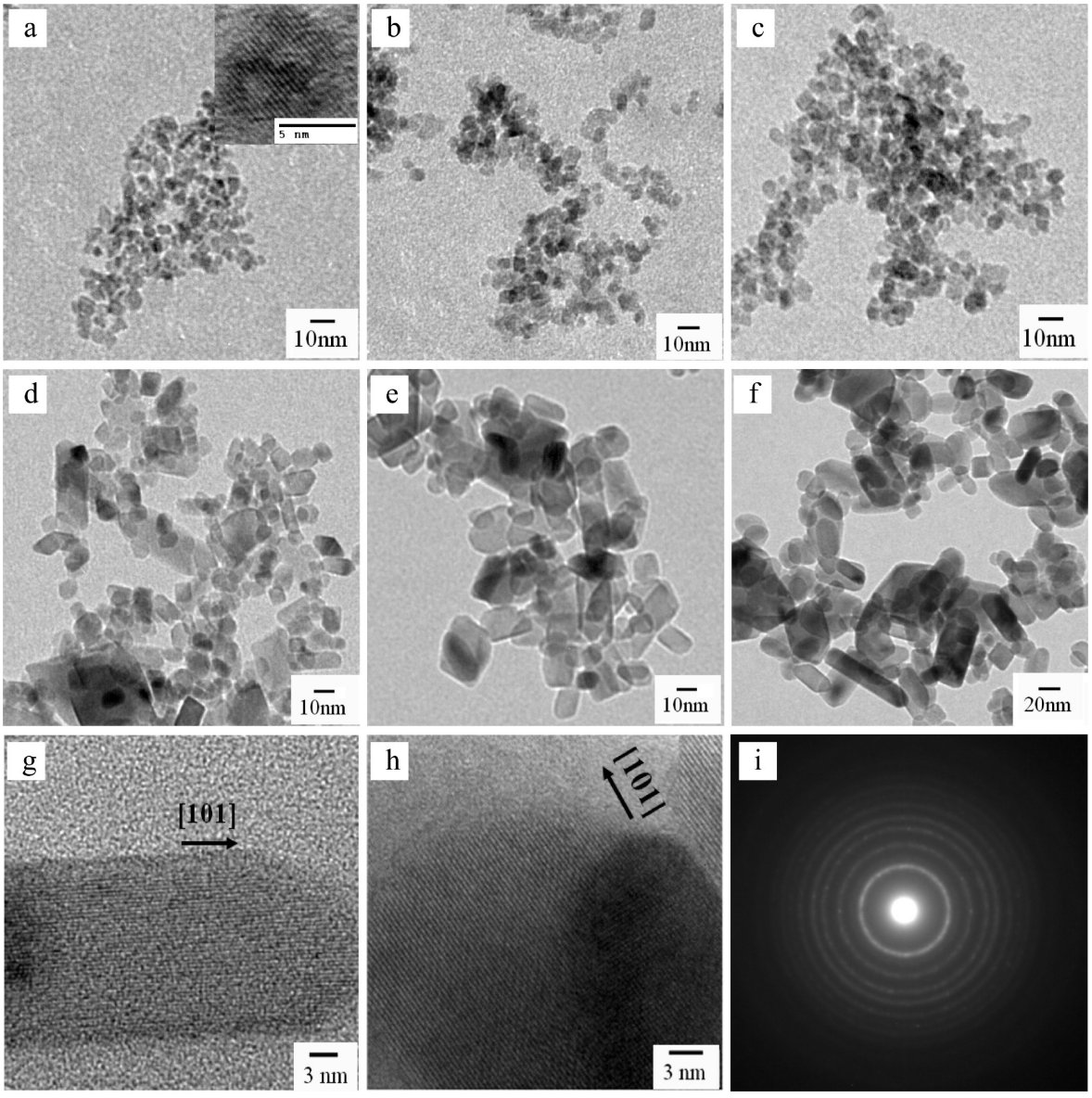

Figure 2. Effect of hydrothermal temperature on the dimension and morphology of TiO_2 nanoparticles, W = 56, hydrothermal for 13 h, (a) 120 °C, (b) 150 °C, (c) 200 °C, (d) 250 °C, (e) 300 °C, (f) 350 °C, (g) 250 °C, (h) 350 °C, and (i) 120 °C.

dx.doi.org/10.1021/sc400328u | ACS Sustainable Chem. Eng. 2014, 2, 288−295

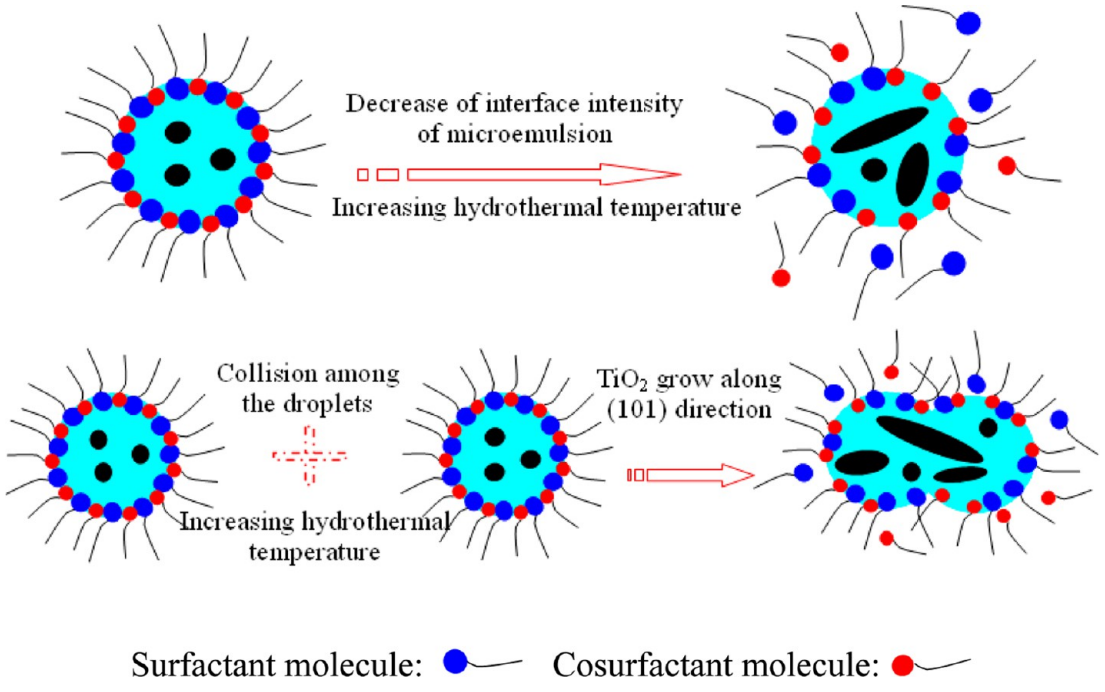

Figure 3. Formation mechanism of TiO_2 nanoparticles at elevated hydrothermal temperature.

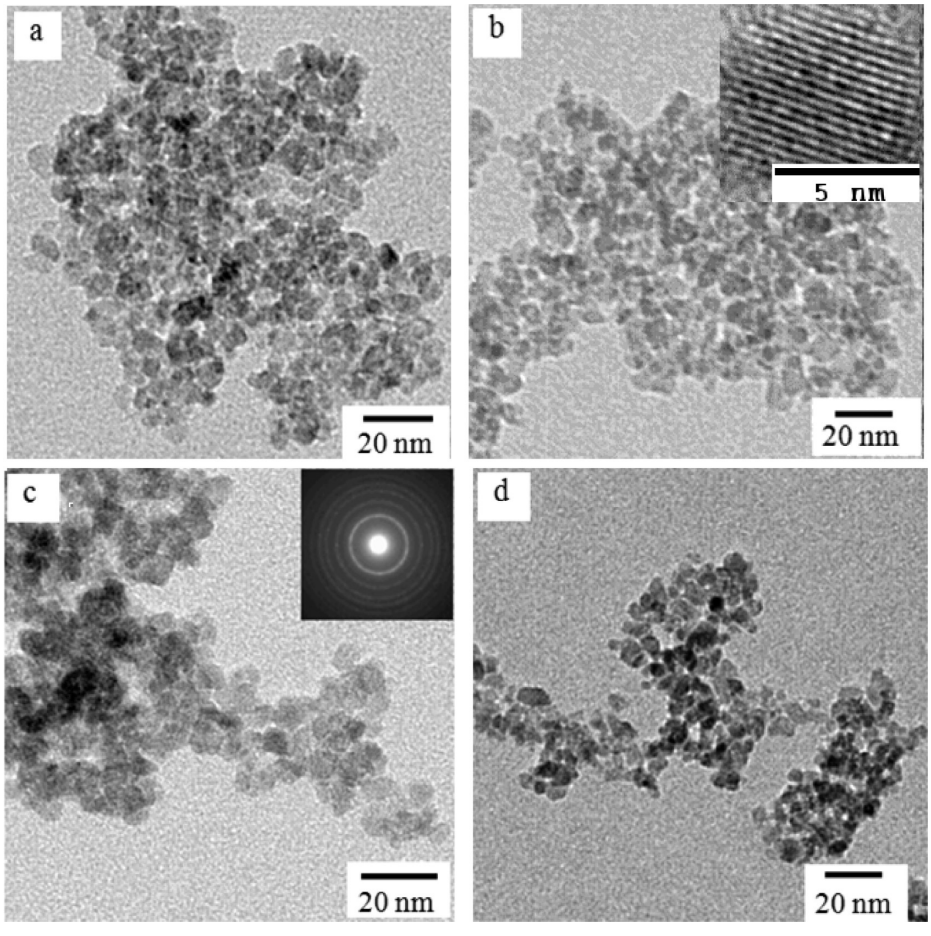

Figure 4. Effect of water content on the morphology of TiO_2 nanoparticles, 1 mL TIP, hydrothermal treatment 120 °C for 13 h, (a) W = 11, (b) W = 22, (c) W = 33.3, and (d) W = 50.

Information), and the materials show an amorphous state and low crystallinity compared with the titania nanoparticles in Figure 2. The results reveal the synergetic effects of the microemulsion interface and hydrothermal treatment on the

dx.doi.org/10.1021/sc400328u | ACS Sustainable Chem. Eng. 2014, 2, 288−295

formation of titania particles with controlled shapes and high crystallinity as well as high photoactivity.

Proposed Formation Mechanism of TiO_2 Nanoparticles. Figure 2 indicates that the particle size is strongly affected by the hydrothermal temperature. The formation mechanism of TiO_2 particles with various morphologies has been proposed based on the decrease in intensity of the microemulsion interface and the increase in coalescence between droplets with increasing hydrothermal temperature, as shown in Figure 3. The thermal motion of surfactant and cosurfactant molecules at the microemulsion interface will intensify, and some molecules may return to the oil phase from the oil−water interface at elevated temperature. These behaviors result in a serious decrease in intensity and rigidity of the microemulsion interface. Accordingly, the controlling effect of the flexible and looser interface on crystal growth becomes weaker,[25,33] which is advantageous for growth of the TiO_2 nuclei along its preferential direction. On the other hand, collision and coalescence between microemulsion droplets strengthen with increasing temperature. These increase the crystal growing velocity and provide larger space for the formation of rod-like TiO_2.

The TiO_2 nanoparticles have also been prepared using microemulsion systems with different water contents (W = 11, 22, 33.3, 50). It can be found that spherical particles with diameters of 5−15 nm are obtained in Figure 4, and their surface area, crystalline size, and photoactivity are comparable with each other (Figure S3, Supporting Information and Table 1). The results may be due to the strong restricting effect of the microemulsion interface on the particle growth at the hydrothermal temperature of 120 °C. It is known that the water in the microemulsion polar core lies between the bound and free state from the MB detection. Thus, the water molecules can combine with headgroup of TritonX-100/hexanol and form a "cage" to control the growth of TiO_2 crystal nucleus. With the temperature higher than 200 °C (250−350), however, the decrease in the interface intensity and collision among the microemulsion droplets can provide a large space and optimal microenvironment for the growth of the titania crystal. Therefore, the mixtures of spherical and rod-shaped particles are obtained at this condition (Figure 2d−f). Combining the morphology evolution process in Figure 2, it can be concluded that both the microemulsion and hydrothermal treatment play crucial roles in the control of particle morphology (Figures 2 and 4), surface area, and crystalline size (Tables 1 and 2), and accordingly the photoactivity

To further study the interaction among the droplets, conductivity measurements on the microemulsion have been performed at different temperatures (Figure S4, Supporting Information). This reveals that the conductivity of the microemulsion with TritonX-100 as surfactant and hexanol as cosurfactant increase with increasing temperature. This can be explained by the activation energy theory, which is the energy required for mass transfer of substances between adhering droplets and for separating the droplets in the "transient fusion−mass transfer−fission" process.[34,35] The association of the droplets occurs, and either the ions or charges are exchanged between droplets. The droplets collision, fusion, and substance exchange accelerate due to an decrease in intensity of the microemulsion interface at high temperature. The enhanced conductivity has been attributed to the formation of chains/clusters of dispersed droplets and mass transfer across the microemulsion interface, which behaves as an electrical conducting constituent in the solution. In this study, the energy required for mass transfer of TiO_2 nuclei and water molecules between adhering droplets decreases at high hydrothermal temperature, and this results in an increase in particle size and formation of rod-shaped products.

Table 2. Physicochemical Properties of TiO_2 Samples from N_2 Desorption Analysis and XRD Results, Effect of Different Hydrothermal Temperature (W = 56, 1 mL TIP)

temperature (°C)	S_{BET} (m^2/g)	V (cm^3/g)	D_{BJH} (Å)	crystalline size (nm)	kinetic constant (min^{-1})
120	225.13	0.46	81.01	8.10	0.0452
150	158.00	0.41	102.70	8.60	0.0256
200	146.35	0.49	136.30	9.90	0.0191
250	90.94	0.50	220.70	15.28	0.0860
300	40.84	0.33	323.20	20.80	0.0865
350	28.44	0.15	380.06	24.33	0.0966
P-25	58.70	0.23	152.91	26.20	0.0889

Total pore volume, V (cm^3/g), obtained from the volume of N_2 adsorption at P/P_0 = 0.995. Average pore diameter, D_{BJH} (nm), estimated using the desorption branch of the isotherm.

N_2 Adsorption/Desorption Analysis. The N_2 adsorption−desorption isotherms and Barrett−Joyner−Halenda (BJH) pore size distributions of all the samples are shown in Figure 5. We can obviously observe that the isotherms of the samples are of classical type IV with H2 hysteresis loops between the adsorption and desorption curves, indicting the existence of ink-bottle-like pore structure with a narrow entrance and large cavity.[8,36] From Figure 5a, the hysteresis loops of the samples prepared at elevated temperature shift to high relative pressure (P/P_0), and its slope becomes steeper. Ordered mesoporous structures are not observed in TEM images, and the mesoporosity is mainly due to the interparticle porosity rather than intraparticle porosity. Therefore, the aggregation of nanoparticles has been considered to be the main reason for the formation of mesoporous structures. The textural and structure parameters of the samples have been summarized in Table 2. With increasing the hydrothermal temperature, the surface area and pore volume decrease significantly, as well as the amount of adsorbed N_2. However, both the crystalline size and average pore size increase gradually. These phenomena can be attributed to the fact that with a decrease in intensity of the microemulsion interface at high hydrothermal temperature, the particle size becomes large due to the crystallization of TiO_2, and subsequently much large crystal growth leads to a significant decrease in the surface area and pore volume of the samples. It is well known that the average pore diameter increases with an increase in TiO_2 crsytalline size, as confirmed by XRD analysis, and the narrow pore size distributions for the samples synthesized at 120 and 150 °C indicate that the pores formed from the assembly of TiO_2 nanoparticles have a similar size in Figure 5b. However, large mean pore size and broad pore size distribution can be observed in the figure with increasing hydrothermal temperature. The results may be ascribed to the disordered arrangement of spherical and rod-like TiO_2 nanoparticles. Furthermore, the block of surfactants remaining in the as-synthesized particles on pore channels can also cause broad pore size distribution.[10]

To further study the blocking influence of the surfactant on particle textural parameters. We have prepared TiO_2 nanoparticles in the same microemulsion at room temperature and

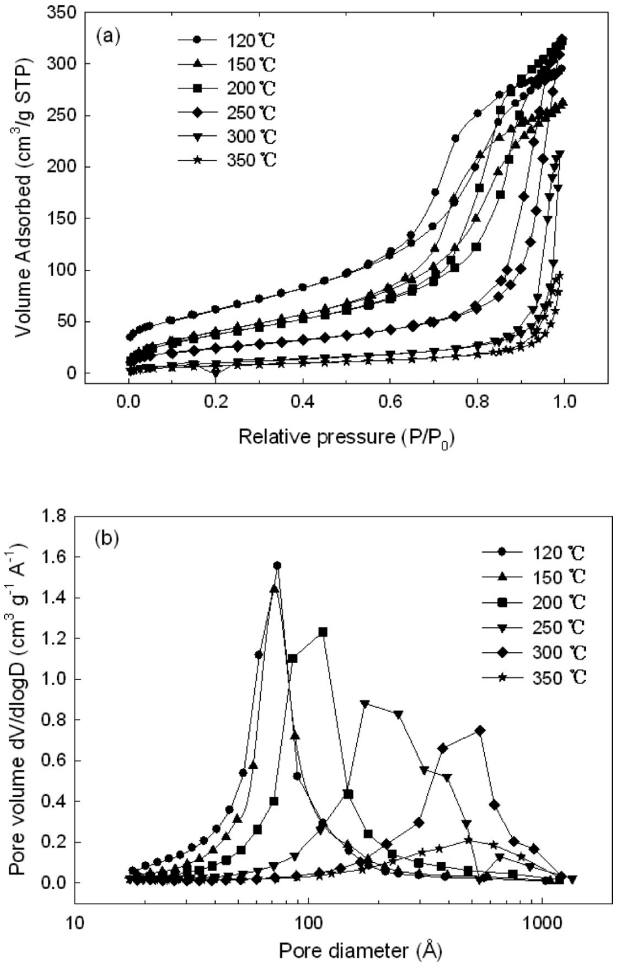

Figure 5. N_2 adsorption−desorption curves and pore size distributions of TiO_2 nanoparticles prepared at different hydrothermal temperatures.

then calcined the samples at different temperatures for 3 h. As shown in Table 3, with increasing the calcination temperature, the BET surface and pore volume of the products increase and then decrease, exhibiting a maximum surface area of 1710.12 m^2/g and a very high pore volume of 1.976 cm^3/g, corresponding to mean pore size of 4.4 nm at 300 °C. The fluctuation can be explained as follows. With increasing the calcination temperature from 150 to 300 °C, the surfactant and cosurfactant molecules adsorbed on the particle surface are removed, and the surface area and pore volume are increased. When the calcination temperature is higher than 300 °C, the two parameters decrease rapidly due to the crystallization of TiO_2, subsequent crystal growth, and collapse of the mesoporous structure, accompanying with a gradual increase in the mean pore diameter and crystalline size. The TiO_2 materials with high surface area and pore volume provide possible applications in the adsorption process and catalyst support. The experiment also reveals the adsorption of the surfactant on the particle surface and the controlling effect on particle growth.

Table 3. Physicochemical Properties of the TiO_2 Samples from N_2 Desorption Analysis and XRD Results, Effect of Different Calcination Temperature (W = 56, 1 mL TIP)

temperature (°C)	S_{BET} (m^2/g)	V (cm^3/g)	D_{BJH} (Å)	crystalline size (nm)	kinetic constant (min^{-1})
150	472.04	0.55	42.40	–	–
200	527.99	0.58	41.28	–	–
250	553.51	0.61	40.24	–	–
300	1710.12	1.98	43.88	–	–
350	339.38	0.44	47.26	9.10	0.0087
500	65.83	0.22	101.30	13.50	0.0228
700	11.04	0.08	263.97	27.30	0.0251

Total pore volume, V (cm^3/g), obtained from the volume of N_2 adsorption at P/P_0 = 0.995. Average pore diameter, D_{BJH} (nm), estimated using the desorption branch of the isotherm.

Photocatalytic Activity of TiO_2 Samples. The photocatalytic activity of the titania samples was examined by measuring the photodegradation of Rhodamine B in an aqueous suspension of titania. To account for the possible decrease in the organic dye concentration due to heat generated from irradiation, a control experiment without any catalyst in the solution was carried out. There is almost no decrease in RhB concentration after 120 min irradiation in the absence of TiO_2, as depicted in Figure 6a. Figure 6b illustrates that the

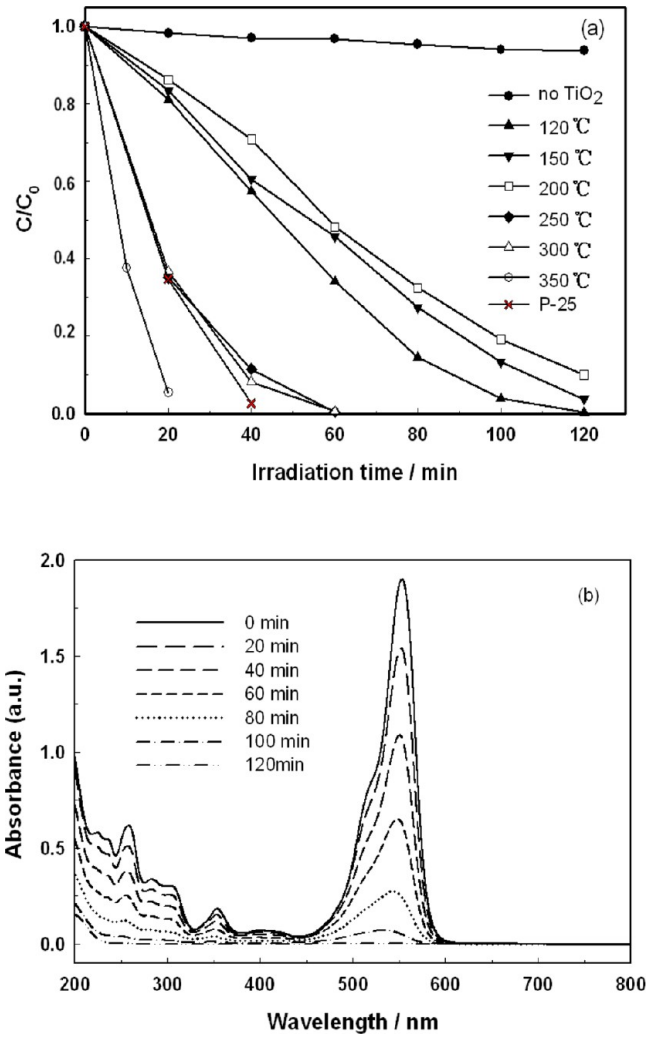

Figure 6. (a) Degradation of RhB using TiO_2 nanoparticles prepared at different hydrothermal temperatures. (b) Variation of RhB concentration in aqueous solution with irradiating time. TiO_2 nanoparticles prepared at 120 °C.

dx.doi.org/10.1021/sc400328u | ACS Sustainable Chem. Eng. 2014, 2, 288−295

UV−vis absorption of RhB decreases gradually with an increase in illumination time, and no any characteristic peaks of RhB are observed after 120 min irradiation. More importantly, there is almost no wavenumber shift for the absorption at 550 nm during the photocatalytic process, proving that the degradation is complete, and no intermediates of the dye are produced during the photodegradation process.[37,38] The results indicate high efficiency of the as-synthesized TiO_2 particles on the degradation of dye pollutant. In plots of $\ln(C/C_0)$ versus UV irradiation time, straight lines are found for all samples, indicating that the degradation of Rhodamine B is a pseudo-first-order process (data not show). It has been commonly accepted that a large surface area means high photoactiviy because many substances can adsorb onto the active sites of the catalyst.[39,40] Furthermore, the small crystalline size corresponds to a more powerful redox ability because the small crystalline size induces a large band gap energy, and mesoporous TiO_2 with smaller pore size is likely to exhibit better photocatalytic activity. However, in our study, the photodecomposition rate constants have been calculated to be 0.0452, 0.0256, and 0.019 min^{-1} for the samples synthesized at hydrothermal temperatures of 120, 150, and 200 °C, respectively, as shown in Table 2, while the samples prepared at 250−350 °C exhibit high values of 0.0860, 0.0865, and 0.096 min^{-1} and are comparable or higher than that of Degussa P-25 (0.088 min^{-1}). The results can be explained in terms of surface area, crystalline size, and crystallinity of the catalyst. At the low-temperature region of 120−200 °C, the weak photoactivity of the particles can be ascribed to their relatively low crystallinity though they have higher surface area and small crystalline size and pore diameter. Additionally, the constants decrease from 0.0452 to 0.019 min^{-1} with increasing hydrothermal temperature. This is because the surface area decreases gradually, which plays a dominant role in this temperature region. At high temperatures of 250−350 °C, the activity of degradation on the dye improves largely though the surface area decreases and crystalline size increases significantly. It is assumed that the crystallinity determines TiO_2 activity at this temperature stage. The high crystallinity results in a reduction in recombination centers such as a kink or defect of oxygen between photoelectrons and positively charged holes. These results suggest that the photocatalytic activity of TiO_2 materials is strongly dependent on the surface area, crystallinity, and crystalline size, and the effects of these factors on the activity are interdependent. The balance between these parameters is important for the preparation of a TiO_2 catalyst with high photoactivity. Furthermore, some TiO_2 samples were also prepared by the calcination method (hydrolysis of TIP in the microemulsion first at room temperature). From Table 3, however, the samples calcined at 150−300 °C show no activity on the degradation of the dye, and the kinetic constants (0.0087−0.025 min^{-1}) of the samples calcined even at high temperature of 350−700 °C are much smaller than those of the catalysts synthesized by the hydrothermal−microemulsion combined route (0.086−0.096 min^{-1}). The results may be due to their amorphous state, low crystallinity, or surface area of the calcined samples (Figure S5, Supporting Information). Therefore, it is feasible to prepare a TiO_2 catalyst with controlled morphology and high performance under the relative mild conditions in this study.

CONCLUSION

Nanosized TiO_2 nanoparticles with improved photocatalytic activity have been prepared via a hydrothermal−microemulsion combined process. With an increase in hydrothermal temperature, the morphology of the tatania materials transits from spherical to rod-shaped particles that show a broad size distribution. The rod-like particles are attributed to the preferred growth of TiO_2 crystal along (101) direction in microemulsion with decreased interface intensity at elevated temperature, which is further proved by the conductivity measurement of the microemulsion. The higher hydrothermal temperature also results in higher crystallinity, crystalline size, and dimension of the prepared particles. The key factors in determining the photocatalytic activity of TiO_2 nanoparticles for decomposition of Rhodamine B are concluded to be the surface area, crystallinity, and crystalline size. Influences of these factors are interdependent. The rod-shaped samples exhibit comparable or higher activity than that of commercial P-25 because of its high crystallinity. The developed hydrothermal−microemulsion route has been demonstrated to be effective for synthesis of titania nanoparticles with controlled morphology and improved activity by varying hydrothermal temperature.

ASSOCIATED CONTENT

Supporting Information

UV−visible absorbance spectra of MB solubilized in microemulsion system with different water content (Figure S1), TiO_2 materials prepared by different calcination method (Figure S2), XRD spectra of TiO_2 nanoparticles prepared in microemulsion with different water contents (Figure S3), effect of temperature on conductivity of the microemulsion system (Figure S4), and XRD patterns of TiO_2 nanoparticles prepared in microemulsion at room temperature and then calcined at different temperatures (Figure S5). This material is available free of charge via the Internet at http://pubs.acs.org.

AUTHOR INFORMATION

Corresponding Authors

*E-mail: lixiangcun@dlut.edu.cn (L.X.). Tel: +86-0411-84986291. Fax: +86-0411-84986291.

*E-mail: hgaohong@dlut.edu.cn (G.H.). Tel: +86-0411-84986291. Fax: +86-0411-84986291.

Notes

The authors declare no competing financial interest.

ACKNOWLEDGMENTS

We are grateful for the National Natural Science Foundation of China (21006008, 21206014), Fundamental Research Funds for the Central Universities (DUT12JN07), Open Fund of Key Laboratory (2012LNSP02), and National Science Fund for Distinguished Young Scholars of China (21125628).

REFERENCES

(1) Tang, X.; Li, D. Evaluation of asphaltene degradation on highly ordered TiO_2 nanotubular arrays via variations in wettability. *Langmuir* **2011**, *27* (3), 1218−1223.

(2) Naik, G. K.; Mishra, P. M.; Parida, K. Green synthesis of Au/TiO_2 for effective dye degradation in aqueous system. *Chem. Eng. J.* **2013**, *229*, 492−497.

(3) Jiang, X.; Wang, T. Influence of preparation method on morphology and photocatalysis activity of nanostructured TiO_2. *Environ. Sci. Technol.* **2007**, *41*, 4441−4446.

(4) Zhang, R.; Tu, B.; Zhao, D. Synthesis of highly stable and crystalline mesoporous anatase by using a simple surfactant sulfuric acid carbonization method. *Chem.—Eur. J.* **2010**, *16* (33), 9977−9981.

(5) Ren, Y.; Chen, M.; Zhang, Y.; Wu, L. Fabrication of rattle-type TiO_2/SiO_2 core/shell particles with both high photoactivity and UV-shielding property. *Langmuir* **2010**, *26* (13), 11391−11396.
(6) Chen, D.; Caruso, R. A. Recent progress in the synthesis of spherical titania nanostructures and their applications. *Adv. Funct. Mater.* **2013**, *23*, 1356−1374.
(7) Li, X. C.; John, V. T.; He, G. H.; Zhan, J. J.; Tan, G.; McPherson, G.; Bose, A.; Sarkar, J. Shear induced formation of patterned porous titania with applications to photocatalysis. *Langmuir* **2009**, *25* (13), 7586−7593.
(8) Kim, D. S.; Han, S. J.; Kwak, S. Y. Synthesis and photocatalytic activity of mesoporous TiO_2 with the surface area, crystallite size, and pore size. *J. Colloid Interface Sci.* **2007**, *316* (1), 85−91.
(9) Zhao, B.; Lin, L.; He, D. Phase and morphological transitions of titania/titanate nanostructures from an acid to an alkali hydrothermal environment. *J. Mater. Chem. A* **2013**, *1*, 1659−1668.
(10) Lee, M.; Amaratunga, P.; Kim, J.; Lee, D. TiO_2 Nanoparticle photocatalysts modified with monolayer-protected gold clusters. *J. Phys. Chem. C.* **2010**, *114*, 18366−18371.
(11) Mohapatra, P.; Mishra, T.; Parida, K. M. Effect of micro-emulsion composition on textural and photocatalytic activity of titania nanomaterial. *Appl. Catal., A* **2006**, *310*, 183−189.
(12) Li W.; Wu, Z.; Wang, J.; Elzatahry, A. A.; Zhao, D. A perspective on mesoporous TiO_2 materials. *Chem. Mater.* dx.doi.org/10.1021/cm4014859.
(13) Liu, R. L.; Ren, Y. J.; Shi, Y. F.; Zhang, F. L.; Zhang, J.; Tu, B.; Zhao, D. Y. Preparation of mesoporous titania thin films with remarkably high thermal stability. *Chem. Mater.* **2008**, *20* (3), 1140−1146.
(14) Pierre, A. C.; Pajonk, G. M. Chemistry of aerogels and their applications. *Chem. Rev.* **2002**, *102*, 4243−4244.
(15) Lu, Z. L.; Lindner, E.; Mayer, H. A. Design and preparation of organic−inorganic hybrid catalysts. *Chem. Rev.* **2002**, *102* (10), 3543−3578.
(16) Pan, L.; Zou, J. J.; Wang, S. B.; Liu, X. Y.; Zhang, X. W.; Wang, L. Morphology evolution of TiO_2 facets and vital influences on photocatalytic activity. *ACS Appl. Mater. Interfaces* **2012**, *4*, 1650−1655.
(17) Jiang, J.; Gu, F.; Shao, W.; Li, C. Fabrication of spherical multi-hollow TiO_2 nanostructures for photoanode film with enhanced light-scattering performance. *Ind. Eng. Chem. Res.* **2012**, *51*, 2838−2845.
(18) Bahadur, J.; Sen, D.; Mazumder, S.; Sastry, P. U.; Paul, B.; Bhatt, H.; Singh, S. G. One-step fabrication of thermally stable TiO_2/SiO_2 nanocomposite microspheres by evaporation-induced self-assembly. *Langmuir* **2012**, *28*, 11343−11353.
(19) Chae, S. Y.; Park, M. K.; Lee, S. K.; Kim, T. Y.; Kim, S. K.; Lee, W. I. Preparation of size-controlled TiO_2 nanoparticles and derivation of optically transparent photocatalytic films. *Chem. Mater.* **2003**, *15* (17), 3326−3331.
(20) Xu, J.; Ge, J. P.; Li, Y. D. Solvthermal synthesis of monodisperse PbSe nanocrystals. *J. Phys. Chem. B.* **2006**, *110* (6), 2497−2501.
(21) Pradhan, S. K.; Reucroft, P. J.; Yang, F.; Dozier, A. Growth of TiO_2 nanorods by metalorganic chemical vapor deposition. *J. Cryst. Growth.* **2003**, *256* (1), 83−88.
(22) Yu, J. C.; Zhang, L.; Li, Q.; Kwong, K. W.; Xu, A. W.; Lin, J. Sonochemical preparation of nanoporous composites of titanium oxide and size-tunable strontium titanate crystals. *Langmuir* **2003**, *19* (18), 7673−7675.
(23) Wu, X.; Jiang, Q. Z.; Ma, Z. F.; Fu, M. Synthesis of titania nanotubes by microwave irradiation. *Solid State Commun.* **2005**, *136* (9), 513−517.
(24) Gressel-Michel, E.; Chaumont, D.; Stuerga, D. From a microwave flash-synthesized TiO_2 colloidal suspension to TiO_2 thin films. *J. Colloid Interface Sci.* **2005**, *285* (2), 674−679.
(25) Li, X. C.; He, G. H.; Xiao, G. K.; Liu, H. J.; Wang, M. Synthesis and morphology control of ZnO nanostructures in microemulsions. *J. Colloid Interface Sci.* **2009**, *333* (2), 465−473.
(26) Inaba, R.; Fukahori, T.; Hamamoto, M.; Ohno, T. Synthesis of nanosized TiO_2 particles in reverse micelle systems and their photocatalytic activity for degradation of toluene in gas phase. *J. Mol. Catal.* **2006**, *260* (1), 247−254.
(27) Lu, C. H.; Wen, M. C. Synthesis of nanosized TiO_2 powders via a hydrothermal microemulsion process. *J. Alloys Compd.* **2008**, *448* (1), 153−158.
(28) Lu, C. H.; Wu, W. H.; Kale, R. B. Microemulsion-mediated hydrothermal synthesis of photocatalytic TiO_2 powders. *J. Hazard. Mater.* **2008**, *154* (1), 649−654.
(29) Yu, J. G.; Su, Y. R.; Cheng, B.; Zhou, M. H. Effects of pH on the microstructures and photocatalytic activity of mesoporous nanocrystalline titania powders prepared via hydrothermal method. *J. Mol. Catal. A: Chem.* **2006**, *258* (2), 104−112.
(30) Lee, M. S.; Park, S. S.; Lee, G. D.; Ju, C. S.; Hong, S. S. Synthesis of TiO_2 particles by reverse microemulsion method using nonionic surfactants with different hydrophilic and hydrophobic group and their photocatalytic activity. *Catal. Today* **2005**, *101* (3), 283−290.
(31) Zhu, D M; Wu, X.; Schelly, Z A. Investigation of the micropolarities in reverse micelles of Triton X-100 in mixed solvents of benzene and n-hexane. *J. Phys. Chem.* **1992**, *96*, 7121−7126.
(32) Qi, L M; Ma, J M. Investigation of the microemulsion microenvironment in nonionic reverse micelles using methyl orange and methylene blue as absorption probes. *J. Colloid Interface Sci.* **1998**, *197*, 36−42.
(33) Usui, H. Surfactant concentration dependence of structure and photocatalytic properties of zinc oxide rods prepared using chemical synthesis in aqueous solutions. *J. Colloid Interface Sci.* **2009**, *336* (2), 667−674.
(34) Paul, S.; Bisal, S.; Moulik, S. P. Physicochemical studies on microemulsions: test of the theories of percolation. *J. Phys. Chem.* **1992**, *96* (2), 896−901.
(35) Li, X. C.; He, G. H.; Zheng, W. J.; Xiao, G. K. Study on conductivity property and microstructure of TritonX-100/alkanol/n-heptane/water microemulsion. *Colloids Surf., A* **2010**, *360* (1−3), 150−158.
(36) Tsai, C. C.; Teng, H. Regulation of the physical characteristics of titania nanotube aggregates synthesized from hydrothermal treatment. *Chem. Mater.* **2004**, *16* (22), 4352−4358.
(37) Wang, Z.; Yang, C.; Liu, T.; Yin, H.; Chen, P.; Wan, D.; Xu, F.; Huang, F.; Lin, J.; Xie, X.; Jiang, M. Visible-light photocatalytic, solar thermal and photoelectrochemical properties of aluminium-reduced black titania. *Energy Environ. Sci.* **2013**, *6*, 3007−3014.
(38) Chen, C.; Zhao, W.; Lei, P.; Zhao, J.; Serpone, N. Photosensitized degradation of dyes in polyoxometalate solutions versus TiO_2 dispersions under visible-light irradiation: Mechanistic implications. *Chem.—Eur. J.* **2004**, *10*, 1956−1965.
(39) Cheng, X.; Chen, M.; Wu, L.; Gu, G. Novel and facile method for the preparation of monodispersed titania hollow spheres. *Langmuir* **2006**, *22* (8), 3858−3863.
(40) Sun, W.; Zhou, S.; You, B.; Wu, L. Facile fabrication and high photoelectric properties of hierarchically ordered porous TiO_2. *Chem. Mater.* **2012**, *24*, 3800−3810.